



## CHAPTER IV

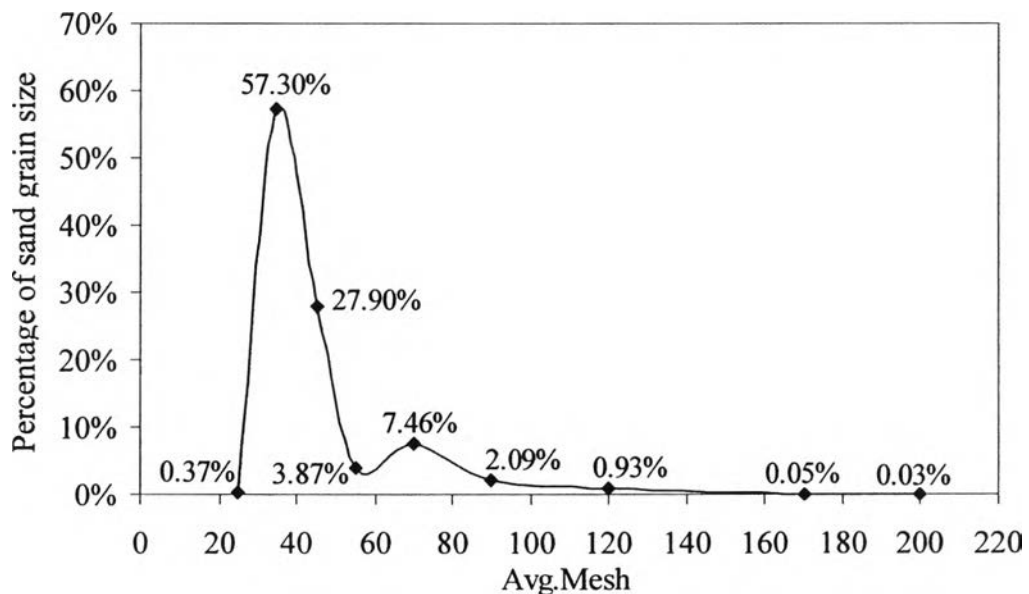
### RESULTS AND DISCUSSION FOR UNCONSOLIDATED POROUS MEDIA

#### 4.1 Analysis of Sand Properties

In this part of the study, the Ottawa sand has been used as a material for sand pack samples which represent the porous media. A syringe of 44.07 cm<sup>3</sup> was used as a cylindrical cell for the sand pack. The porous media, therefore, was unconsolidated with high permeability and porosity.

##### 4.1.1 Sand Grain Size Distribution

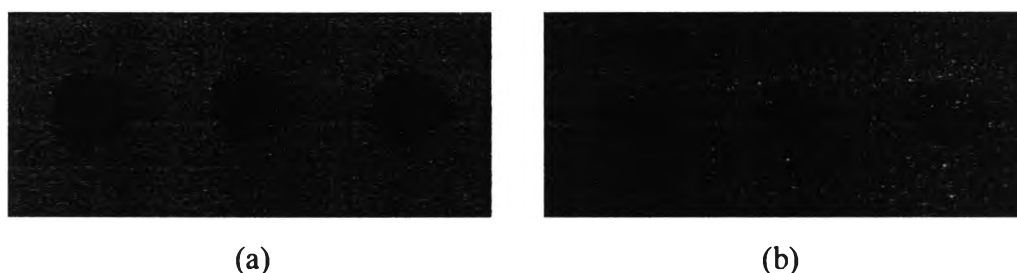
The sand was sieved using specific sized screens in the range of 20-200 mesh. The sand contained a maximum percentage of 57.30% by weight in the range of 30-40 mesh which was equivalent to a grain diameter range from 0.595 to 0.417 mm.



**Figure 4.1** Ottawa sand grain size distribution

#### 4.1.2 Silica Sand Wettability Alteration

The wettability of sand was altered by using AquaSil™ solution. AquaSil™ forms silanol polymers in solution that react with the silanols (Si-OH) on the glass surface. Covalent bonds are formed among the hydroxyls on the glass, so the surface becomes hydrophobic and is able to repel water (AquaSil™ and SurfaSil™ Sili-conizing Fluids data sheet, 2003). In order to distinguish the wettability of sand, colored water was dropped on a layer of sand in a glass container as shown in Figure 4.2. For water-wet sand, colored water rapidly imbibed through the sand. In contrast, the colored water formed like a drop first and gradually spread on the oil-wet sand.



**Figure 4.2** Wettability visualization for (a) Water-wet sand (b) Oil-wet sand

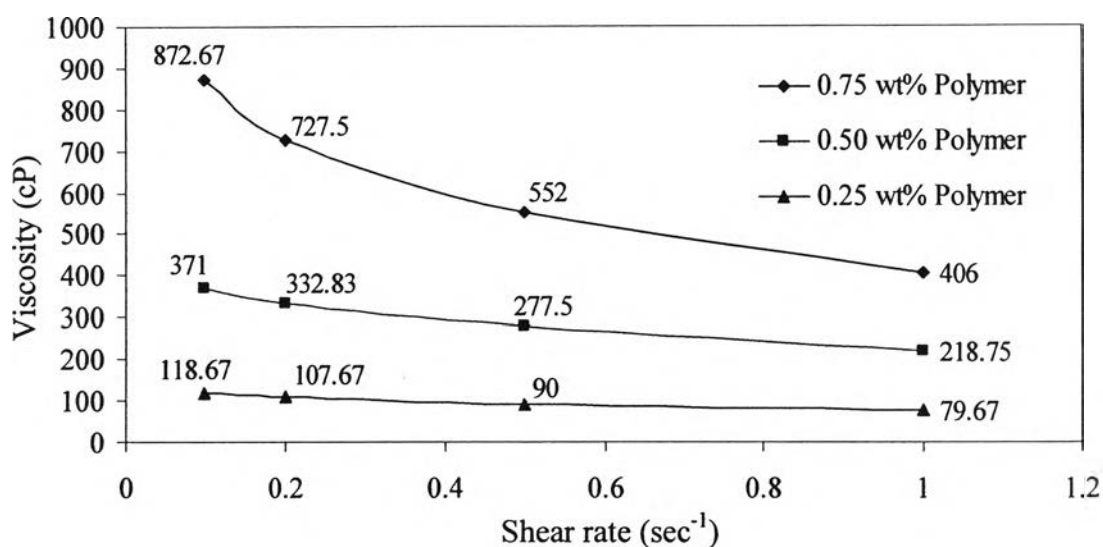
#### 4.2 Analysis of Fluid Properties

In this experiment, Pycnometer 10 ml has been used to determine the density of Fluorolube FS-5. The LVF Viscometer with 4 speeds (6, 12, 30, and 60 RPM i.e. shear rate of 0.1, 0.2, 0.5, and 1  $\text{sec}^{-1}$  respectively) has been used to determine the viscosity of the fluids.

In this experiment, deionized water and Fluorolube FS-5 are Newtonian fluids (constant viscosity). The deionized water has density of 1 g/ml and a viscosity of 1 cP at room temperature ( $\sim 25^\circ\text{C}$ ). The density and viscosity of Fluorolube FS-5 are 1.89 g/ml, and 25.8 cP respectively at room temperature ( $\sim 25^\circ\text{C}$ ). The interfacial tension between deionized water and oil is 43.5 dynes/cm.

In contrast, a polymer that is a non-Newtonian fluid gives a viscosity depending on shear rate. The polymer (HPAM) concentrations of 0.25 wt%, 0.50 wt%, and 0.75 wt% i.e. 2,500 ppm, 5,000 ppm, and 7,500 ppm respectively were investigated. The relationship between viscosity and shear rate ( $\text{sec}^{-1}$ ) for each concentra-

tion of polymer is shown in Figure 4.3. From the figure, the viscosities decrease with the shear rate, which is a property of a shear-thinning fluid. The viscosity at each shear rate increases as the polymer concentration increases. The shear-thinning viscosity behavior becomes less noticeable as the concentration of the polymer decreases. All measurements were made at room temperature ( $\sim 25^\circ\text{C}$ ).



**Figure 4.3** Viscosity of polymer

### 4.3 Waterflooding Process













Three waterflooding experiments were conducted. Properties of the sand pack sample before flood testing such as pore volume, porosity, and permeability are shown in Table 4.1. The average pore volume and porosity for three samples were 15.38 ml and 34.89 %, respectively. The absolute permeability was in the range of 18,630-34,230 mD. All experiments were undertaken at room temperature ( $\sim 25^\circ\text{C}$ ).

**Table 4.1** Properties of sand pack sample before waterflooding tests

| Sample            | Pore Volume | Porosity | Permeability |
|-------------------|-------------|----------|--------------|
| Waterflooding # 1 | 14.57 ml    | 33.07 %  | -            |
| Waterflooding # 2 | 15.16 ml    | 34.41 %  | 18,630 mD    |
| Waterflooding # 3 | 16.39 ml    | 37.20 %  | 34,230 mD    |

Since MRI in this case detects the signal from the fluorine element, the imaging from MRI show the signal intensity of Fluorolube FS-5 (white areas) and water (dark areas). The oil to water viscosity ratio,  $\mu_o/\mu_w$ , is 25.8 at 25 °C. This oil/water viscosity ratio is  $> 1$  which leads to an unstable displacement ( $M > 1$ ). The series of images for each experiment represents flooding processes at difference volumes of waterflooding as shown in Table 4.2.

**Table 4.2** Images of porous media during waterflooding tests

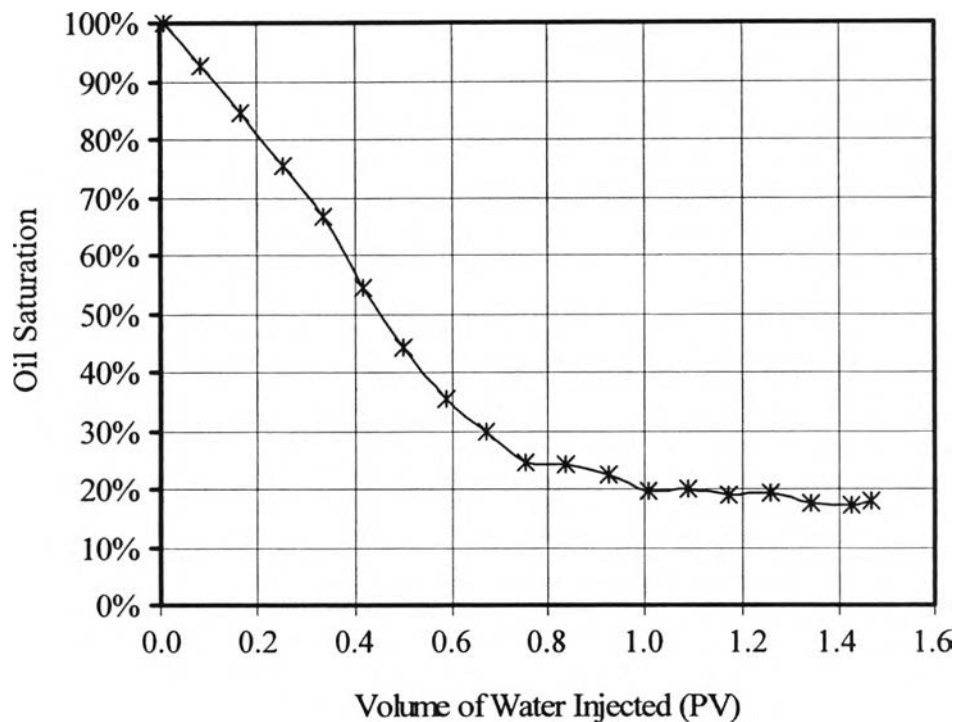
| Sample             | Oil saturation before flooding | Total volume of flooding | Images at each PV                                                                            |                                                                                               |                                                                                                |                                                                                                |
|--------------------|--------------------------------|--------------------------|----------------------------------------------------------------------------------------------|-----------------------------------------------------------------------------------------------|------------------------------------------------------------------------------------------------|------------------------------------------------------------------------------------------------|
| Water-flooding # 1 | 94.90 vol%                     | 36 ml,<br>2.47 PV        | <br>0.021  | <br>0.206  | <br>0.412  | <br>0.824  |
| Water-flooding # 2 | 83.51 vol%                     | 32.32 ml,<br>2.13 PV     | <br>0.010 | <br>0.203 | <br>0.406 | <br>0.812 |
| Water-flooding # 3 | 84.05 vol%                     | 24.06 ml,<br>1.47 PV     | <br>0.008 | <br>0.168 | <br>0.419 | <br>0.755 |

In Waterflooding # 1, 36 ml of water (2.47 PV) was injected at a constant flow rate of 0.1 ml/min. This first experiment showed that the injected water was heterogeneously distributed along the sand pack. An initial oil saturation of 94.90 % was observed before the waterflooding process. As shown in the first image (0.021 PV), some areas presented higher water saturation (dark areas) than others. This could be the result of sand pack permeability heterogeneities formed during the preparation of

the sand pack. The heterogeneities in this sample resemble linear sand beds in series. The oil phase was flooded in pockets caused by the unstable water-drive front until it reached the residual oil saturation ( $S_{or}$ ) of 42.8 % according to MRI.

For Waterflooding # 2, 32.32 ml of water (2.13 PV) at a constant flow rate of 0.05 ml/min was injected. The initial oil saturation of 83.51 % was measured. The channeling and/or fingering (the unfavorable water saturation profile) of water was clearly detected from the images during early stages of the waterflooding process. Table 4.2 shows the evolution of water channeling in the sand pack until it reached a  $S_{or}$  of 31.3 % based on the MRI technique.

Waterflooding # 3 was prepared following the same methodology as before. Therefore, this experiment can compare with other polymer flooding samples. The permeability of 34,230 mD for this sand pack is almost twice that of Waterflooding #2. Thus, it is expected that this high permeability value may favour oil recovery. Before waterflooding, the initial oil saturation was 84.05 %. Then, 24.06 ml of water (1.47 PV) was injected at a constant flow rate of 0.06 ml/min. From the images, water channeling was detected at the beginning of the waterflooding process (0.008 PV). This water drive process gives an oil recovery of 79.7% based on a material balance. The residual oil saturation ( $S_{or}$ ) from a material balance and MRI measurement is 20.3 % and 17.8 %, respectively. The difference between the  $S_{or}$  values obtained from the MRI technique with respect to the material balance is only 2.5%. Figure 4.4 illustrates direct MRI monitoring of the oil saturation in the sample during the waterflooding process. In these experimental conditions, it can be concluded that the waterflooding process was far from the ideal piston-like displacement.

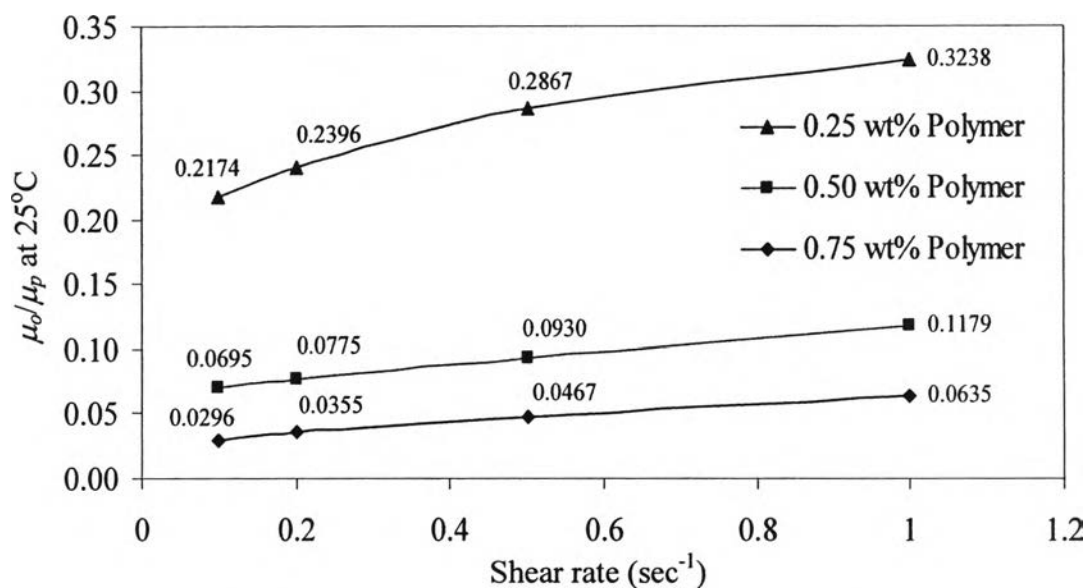


**Figure 4.4** Residual oil saturation ( $S_{or}$ ) profile from MRI for Waterflooding # 3

#### 4.4 Polymer Flooding Process

Polymer flooding processes were investigated in three concentrations of 0.25 wt%, 0.50 wt%, and 0.75 wt% (2,500 ppm, 5,000 ppm, and 7,500 ppm respectively) for water-wet sand and oil-wet sand. A constant flow rate of 0.06 ml/min was used for all experiments. Fluorolube FS-5 was used as the oil phase to distinguish between the oil phase and the aqueous phase. Material balances and MRI were used in these experiments to monitor the efficiency of the flooding process.

The viscosity of the polymer is important in improving the mobility ratio,  $M$ . The oil/polymer viscosity ratio,  $\mu_o/\mu_p$  is shown in Figure 4.5. These oil/polymer viscosity ratios are  $< 1$  for all concentrations of polymer which lead to a favorable mobility ratio ( $M < 1$ ) and a more uniform displacement front.



**Figure 4.5** Oil/polymer viscosity ratio,  $\mu_o/\mu_p$  at 25°C

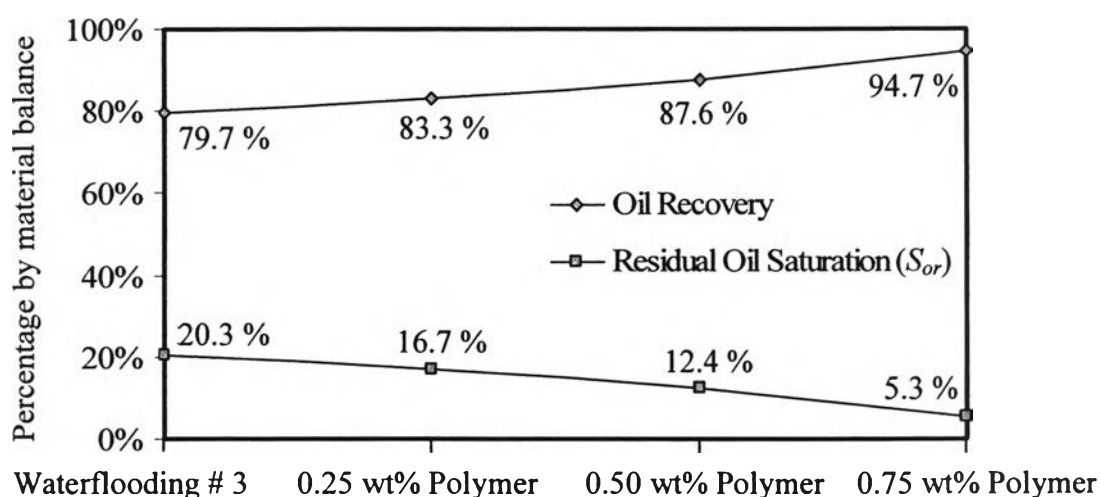
#### 4.4.1 Water-wet sand

This series of experiments consists of four sand pack tests. Three different concentrations of polymer were used for three flooding processes and one water-flooding test (Waterflooding # 3) that represented 0 wt% of polymer concentration. Table 4.3 shows the properties of the sand pack samples before the flood testing, i.e. pore volume, porosity, and permeability. The average pore volume and porosity for the four samples were 16.03 ml and 36.37 %, respectively. The absolute permeability was in the range of 9,400-34,230 mD. All experiments were carried out at room temperature (~25 °C).

**Table 4.3** Properties of sand pack samples before flood testing for water-wet sand

| Water-wet sand sample | Pore Volume | Porosity | Permeability |
|-----------------------|-------------|----------|--------------|
| Waterflooding # 3     | 16.39 ml    | 37.20 %  | 34,230 mD    |
| 0.25 wt% Polymer      | 15.65 ml    | 35.52 %  | 9,400 mD     |
| 0.50 wt% Polymer      | 16.49 ml    | 37.42 %  | 17,340 mD    |
| 0.75 wt% Polymer      | 15.57 ml    | 35.34 %  | 19,920 mD    |

From material balance measurements, the percentage of oil recovery reached the value of 79.68 % for Waterflooding # 3. This percentage increased continuously with the concentration of polymer in the injected water until it reached a maximum value of 94.67 % for 0.75 wt% of polymer concentration as shown in Figure 4.6.



**Figure 4.6** Comparison of oil recovery and  $S_{or}$  by material balance for water-wet sand

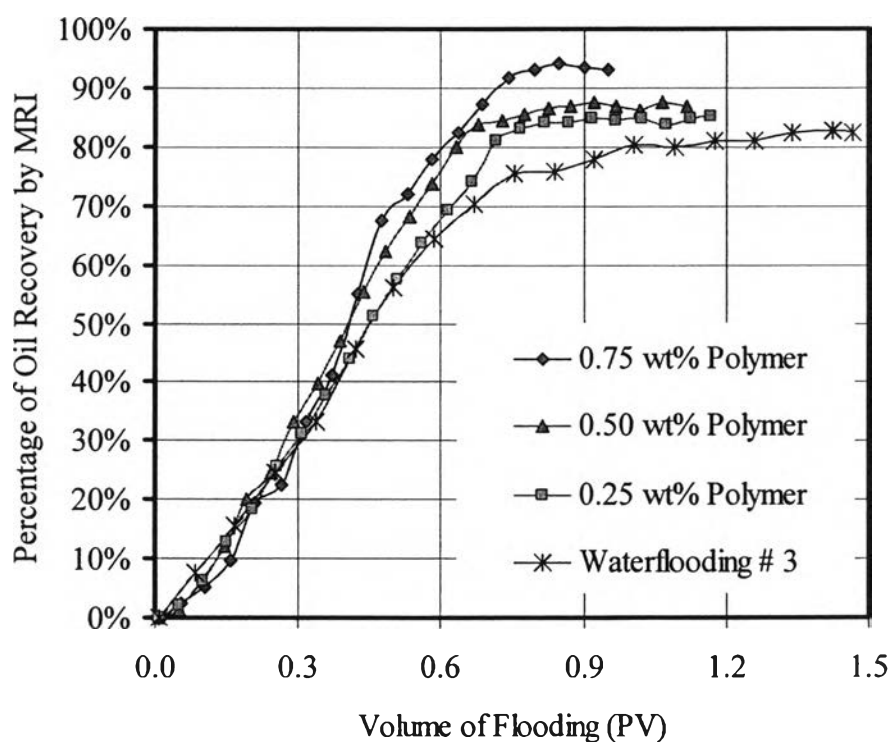
The comparison of residual oil saturation ( $S_{or}$ ) from the material balance and MRI technique is shown in Table 4.4. The largest deviation of 2.5 % was obtained from Waterflooding # 3.

**Table 4.4** Residual oil saturation ( $S_{or}$ ) after flood testing for water-wet sand

| Water-wet sand sample | Residual oil saturation ( $S_{or}$ ) |                  | % Deviation |
|-----------------------|--------------------------------------|------------------|-------------|
|                       | Material balance                     | Imaging from MRI |             |
| Waterflooding # 3     | 20.3 %                               | 17.8 %           | 2.5 %       |
| 0.25 wt% Polymer      | 16.7 %                               | 15.0 %           | 1.7 %       |
| 0.50 wt% Polymer      | 12.4 %                               | 13.1 %           | 0.7 %       |
| 0.75 wt% Polymer      | 5.3 %                                | 6.9 %            | 1.6 %       |



Residual oil saturation was tracked by the integral total MRI signal from the sample during the flooding process. Figure 4.7 shows the oil recovery profiles based on the residual oil saturation in the sample measured by MRI. The figure shows the efficiency of each flooding process, which are Waterflooding # 3 and three concentrations of polymer flooding. In the first stage of flooding (0-0.3 PV), all displacement profiles have the same slope. This implies the polymer does not affect the rate of flooding in this first stage. The oil recoveries keep increasing with different rate. At 0.6 PV, the oil recovery of 0.75 wt% polymer flooding was 15% higher than Waterflooding # 3. The last point of each profile shows the total volume of flooding for each displacement test.

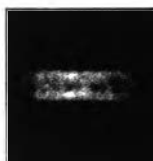
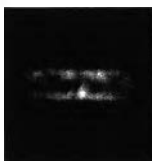

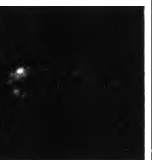
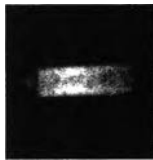
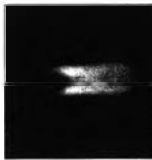
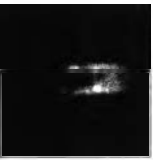


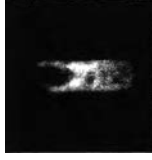



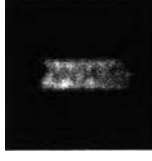




**Figure 4.7** Oil recovery profile from MRI for water-wet sand

The oil saturation before flooding, the total volume of flooding, and the series of imaging from MRI for the different sand pack displacement processes are shown in Table 4.5. The average oil saturation before flooding for four sand pack

tests was 83.10 vol%. The images show the signal intensity of Fluorolube FS-5 (white areas) and polymer (dark areas).

**Table 4.5** Images of porous media during flood testing for water-wet sand

| Sample             | Oil saturation before flooding | Total volume of flooding | Images at each PV                                                                            |                                                                                               |                                                                                                |                                                                                                |
|--------------------|--------------------------------|--------------------------|----------------------------------------------------------------------------------------------|-----------------------------------------------------------------------------------------------|------------------------------------------------------------------------------------------------|------------------------------------------------------------------------------------------------|
| Water-flooding # 3 | 84.05 vol%                     | 24.06 ml,<br>1.47 PV     | <br>0.008   | <br>0.168   | <br>0.419   | <br>0.755   |
| 0.25 wt% Polymer   | 88.17 vol%                     | 18.24 ml,<br>1.16 PV     | <br>0.010 | <br>0.205 | <br>0.409 | <br>0.613 |
| 0.50 wt% Polymer   | 78.11 vol%                     | 18.40 ml,<br>1.12 PV     | <br>0.010 | <br>0.194 | <br>0.388 | <br>0.582 |
| 0.75 wt% Polymer   | 82.08 vol%                     | 14.85 ml,<br>0.95 PV     | <br>0.011 | <br>0.212 | <br>0.424 | <br>0.742 |

Waterflooding # 3 represents the 0 wt% of polymer concentration in the injected water. The permeability measured for this sand pack was 34,230 mD, which is the highest permeability value compared with other sand pack tests in these series of polymer flooding processes. However, the oil viscosity to water viscosity ratio,  $\mu_o/\mu_w$ , is 25.8 at 25°C. This oil/water viscosity ratio is > 1 and comparatively higher

than the oil/polymer viscosity ratio. This leads to an unfavorable displacement ( $M > 1$ ) and fingering of water. In this case, 24.06 ml of water (1.47 PV) was injected at a constant flow rate of 0.06 ml/min. This is the highest total volume of the injected water compared with the polymer flooding displacement tests. The final oil recovery determined from MRI for this waterflooding was 82.2%. From the series of images presented in Table 4.5, the water fingering is clearly observed during the waterflooding process.

The injection of 18.24 ml of polymer solution (1.12 PV) at a constant flow rate of 0.06 ml/min was used in the 0.25 wt% polymer flooding process. The oil/polymer viscosity ratio,  $\mu_o/\mu_p$ , was in the range of 0.2174 – 0.3238 measured from the shear rate of 0.1 to 1  $\text{sec}^{-1}$  at 25 °C. An initial oil saturation of 88.17% was observed before the polymer flooding process. The oil was displaced by polymer solution in a more uniform manner than in the waterflooding displacement. However, the polymer penetrated through the center of sample at 0.409 PV, which showed the unstable displacement front. Although the permeability of this sample was comparatively low at 9,400 mD, the final oil recovery calculated from MRI was 85.0%. The polymer improved the viscosity of the displacing water, making the flooding process more effective.

For 0.50 wt% Polymer, the injection of 18.40 ml of polymer solution (1.12 PV) at a constant flow rate of 0.06 ml/min was used. The oil/polymer viscosity ratio,  $\mu_o/\mu_p$ , was in the range of 0.0695 – 0.1179 measured from the shear rate of 0.1 to 1  $\text{sec}^{-1}$  at 25 °C. An initial oil saturation of 78.11% was measured. The unstable displacement was detected at an early stage. Nevertheless, the image showed a more uniform displacement front at 0.388 PV. This polymer flooding process gives a final oil recovery of 86.9% based on MRI measurement which is higher than the 0.25 wt% Polymer by 1.9%.

0.75 wt% Polymer is the highest concentration of polymer flooding process in these series of polymer displacements. The oil/polymer viscosity ratio,  $\mu_o/\mu_p$ , was in the range of 0.0296 – 0.0635 measured from the shear rate of 0.1 to 1  $\text{sec}^{-1}$  at 25 °C. This ratio is the lowest range compared with other polymer concentrations, which leads to the favorable mobility ratio between the injected polymer solution and the

oil phase. The injection of 14.85 ml of polymer solution (0.95 PV) at a constant flow rate of 0.06 ml/min was used in this experiment. The initial oil saturation of 82.08 % was measured before the polymer flooding process. The uniform displacement front was clearly observed from the images since the beginning of polymer flooding process (0.212 PV). The oil phase was flooded as a piston-like displacement until it reached the final oil recovery of 93.1 % based on MRI measurements.

#### 4.4.2 Oil-wet sand

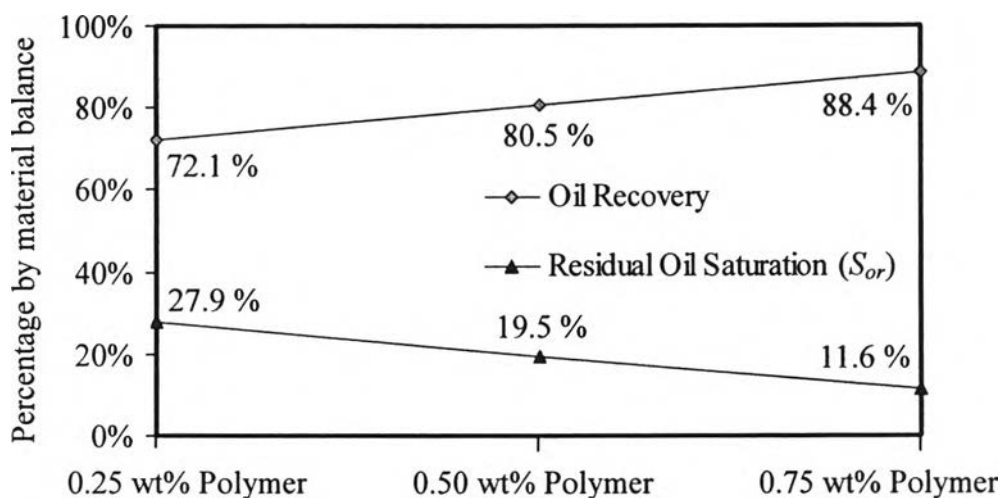
Three different concentrations of polymer in the injected water were used in oil-wet sand pack displacement experiments. Table 4.6 shows the properties of the sand packs before flood testing, i.e. pore volume, porosity, and permeability. The average pore volume and porosity for the three sand packs were 15.52 ml and 35.21 %, respectively. The absolute permeability was in the range of 18,300-30,990 mD. All displacement experiments were carried out at room temperature ( $\sim 25^{\circ}\text{C}$ ).

**Table 4.6** Properties of sand pack samples before flood testing for oil-wet sand

| Oil-wet sand sample | Pore Volume | Porosity | Permeability |
|---------------------|-------------|----------|--------------|
| 0.25 wt% Polymer    | 14.95 ml    | 33.92 %  | 30,990 mD    |
| 0.50 wt% Polymer    | 15.44 ml    | 35.04 %  | 24,680 mD    |
| 0.75 wt% Polymer    | 16.16 ml    | 36.67 %  | 18,300 mD    |

Due to the wettability of the sand (oil-wet sand), it is expected that the oil will occupy the small pores and contact the majority of the sand surface. This leads to less oil recovery compared with oil recovery in water-wet sand. As shown in Figure 4.8, the percentage of the final oil recovery from a material balance was 72.1 % for 0.25 wt% of polymer concentration in the injected water. The percentage of oil recovery continuously increased with the polymer concentration until it reached a maximum value of 88.4 % for 0.75 wt% of polymer concentration in the injected water. For the same concentration of polymer in the injected water, the oil recovery for

the oil-wet sand pack displacement tests is lower than the oil recovery in the water-wet sand pack displacement tests.



**Figure 4.8** Comparison of oil recovery and  $S_{or}$  by material balance for oil-wet sand

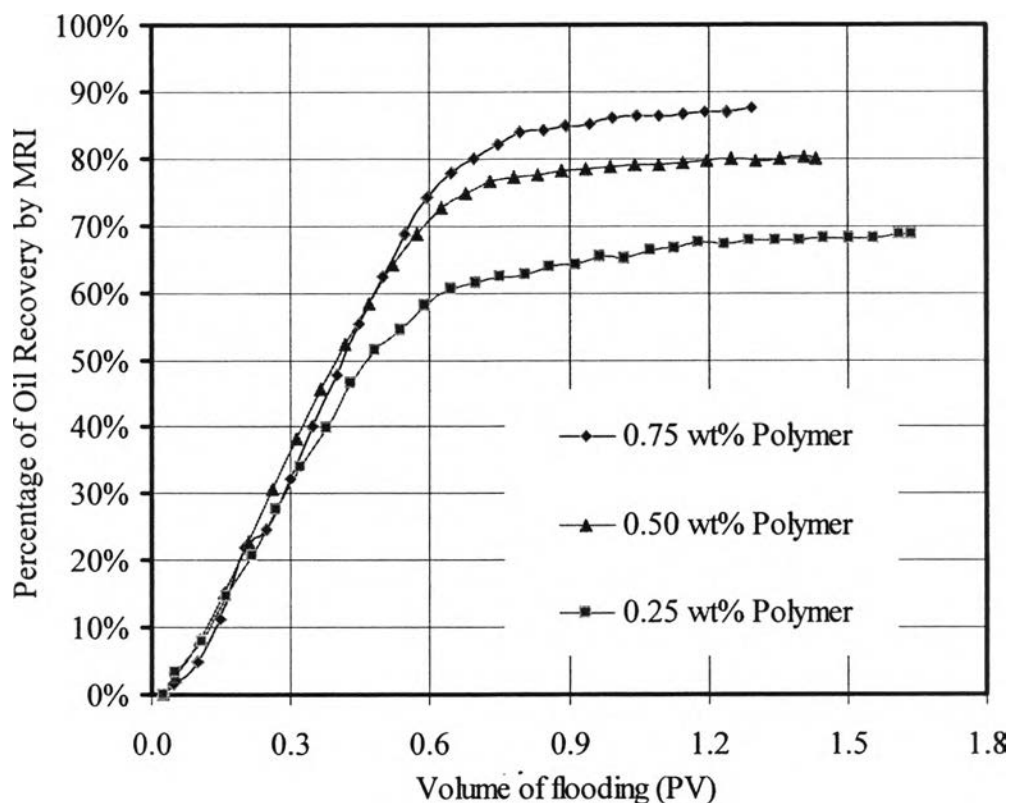
Table 4.7 shows the comparison of residual oil saturation ( $S_{or}$ ) from material balances and the MRI technique. The largest deviation of 3.5 % was obtained from the 0.25 wt% Polymer experiment.

**Table 4.7** Residual oil saturation ( $S_{or}$ ) after flood testing for oil-wet sand

| Oil-wet sand sample | Residual oil saturation ( $S_{or}$ ) |                  | % Deviation |
|---------------------|--------------------------------------|------------------|-------------|
|                     | Material balance                     | Imaging from MRI |             |
| 0.25 wt% Polymer    | 27.9 %                               | 31.4 %           | 3.5 %       |
| 0.50 wt% Polymer    | 19.5 %                               | 19.9 %           | 0.4 %       |
| 0.75 wt% Polymer    | 11.6 %                               | 12.6 %           | 1.0 %       |

Displacement efficiencies in terms of oil recovery profiles calculated by the MRI technique for three different polymer concentrations in polymer flooding processes are shown in Figure 4.9. The profiles have the same trend as polymer flooding processes for water-wet sand. The polymer does not affect the rate of flooding in the









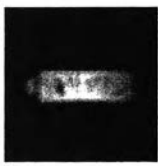
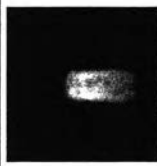
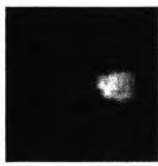

first stage (0-0.3 PV). 0.75 wt% Polymer had a higher rate of oil recovery than the other polymer displacement tests. At 0.9 PV, all of the samples nearly reached the maximum rate of oil recovery. The oil recovery for 0.75 wt% Polymer is greater than 0.25 wt% Polymer by 18.8 %.



**Figure 4.9** Oil recovery profile from MRI for oil-wet sand

Table 4.8 shows the oil saturation before flooding, the total volume of flooding and the series of imaging from MRI for different polymer flooding processes. The average oil saturation before flooding for oil-wet sand samples was 76.63 vol%. This initial oil saturation is lower than water-wet sand packs by 6.47 %. In the oil-wet sand packs, some traps of residual water before the flooding process were observed. The white areas in the images show the signal intensity from Fluorolube FS-5.

**Table 4.8** Images of porous media during flood testing for oil-wet sand

| Sample           | Oil saturation before flooding | Total volume of flooding | Images at each PV                                                                            |                                                                                               |                                                                                                |                                                                                                |
|------------------|--------------------------------|--------------------------|----------------------------------------------------------------------------------------------|-----------------------------------------------------------------------------------------------|------------------------------------------------------------------------------------------------|------------------------------------------------------------------------------------------------|
| 0.25 wt% Polymer | 74.44 vol%                     | 24.49 ml, 1.64 PV        | <br>0.027   | <br>0.269   | <br>0.537   | <br>0.967   |
| 0.50 wt% Polymer | 86.31 vol%                     | 22.08 ml, 1.43 PV        | <br>0.026  | <br>0.260  | <br>0.520  | <br>0.936  |
| 0.75 wt% Polymer | 69.15 vol%                     | 20.88 ml, 1.29 PV        | <br>0.025 | <br>0.249 | <br>0.497 | <br>0.870 |

For the first polymer flooding experiment, a total volume of 24.49 ml (1.64 PV) of 0.25 wt% polymer solution was injected at a constant flow rate of 0.06 ml/min. The oil/polymer viscosity ratio,  $\mu_o/\mu_p$ , was in the range of 0.2174 – 0.3238 measured from the shear rate of 0.1 to 1  $\text{sec}^{-1}$  at 25 °C. The initial oil saturation of 74.44 % was observed before the polymer flooding process. From the image, the disconnected nonwetting phase saturations, i.e. water, were clearly detected in the first image. Then, the polymer solution flooded the oil that surrounded a trap of water. Some of the oil was left behind the trap of water as shown after the injection of 0.537 PV. Oil recovery, from the MRI measurement, was 68.6 %.

In the second polymer displacement test, 22.08 ml (1.43 PV) at a concentration of 0.50 wt% polymer solution was injected at a constant flow rate of 0.06 ml/min. The oil/polymer viscosity ratio,  $\mu_o/\mu_p$ , was in the range of 0.0695 – 0.1179 measured from the shear rate of 0.1 to 1  $\text{sec}^{-1}$  at 25 °C. An initial oil saturation of

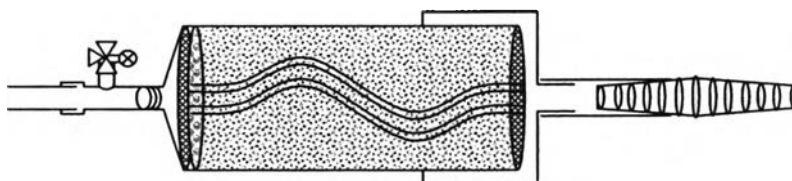
86.31 % was measured. This oil saturation before flooding is higher than 0.25 wt% Polymer sample by 11.87 %. The first image shows agreement since a few traps of water were detected. Then, the oil was flooded by the polymer solution in a more uniform manner. However, significant amounts of residual oil saturations were observed from the images as shown in the image after the injection of 0.520 PV. Finally, the oil recovery based on the MRI technique was 80.1 %.

The last polymer displacement test, 0.75 wt% polymer solution was injected by a volume of 20.88 ml (1.29 PV) at a constant flow rate of 0.06 ml/min. The oil/polymer viscosity ratio,  $\mu_o/\mu_p$ , was in the range of 0.0296 – 0.0635 measured from the shear rate of 0.1 to 1  $\text{sec}^{-1}$  at 25 °C. This ratio is the lowest range since the concentration of polymer is the highest. This leads to a more effective EOR process due to the favorable mobility ratio between the injected polymer solution and the oil bank. An initial oil saturation of 69.15 % was measured before polymer flooding. Again, the traps of residual water were observed at the beginning stage. The images from MRI showed the ideal piston-like displacement along the flooding process. Small amounts of residual oil saturation were detected at the end of the sample. This polymer flooding process gave an oil recovery of 87.4 % calculated from MRI measurement.

#### 4.5 Channel System

Four waterflooding experiments of polymer gel treatment in channel systems were conducted. The Ottawa sand (water-wet sand) was used as a material for the matrix in porous media. The sand was sieved using a specific sized screen in the range of 40-100 mesh, which was equivalent to a grain diameter range from 0.417 mm to 0.150 mm. A syringe of 37.17  $\text{cm}^3$  (2.6 cm in diameter and 7 cm in length) was used as a cylindrical cell for the sand pack. The strongly water-wet glass channel of 0.4  $\text{cm}^3$  which had an inside and outside diameter of 0.23 and 0.41 cm, respectively and a length of 9.5 cm was placed in the center of the sand unit as shown in Figure 4.10.





**Figure 4.10** Schematic of the channel arrangement

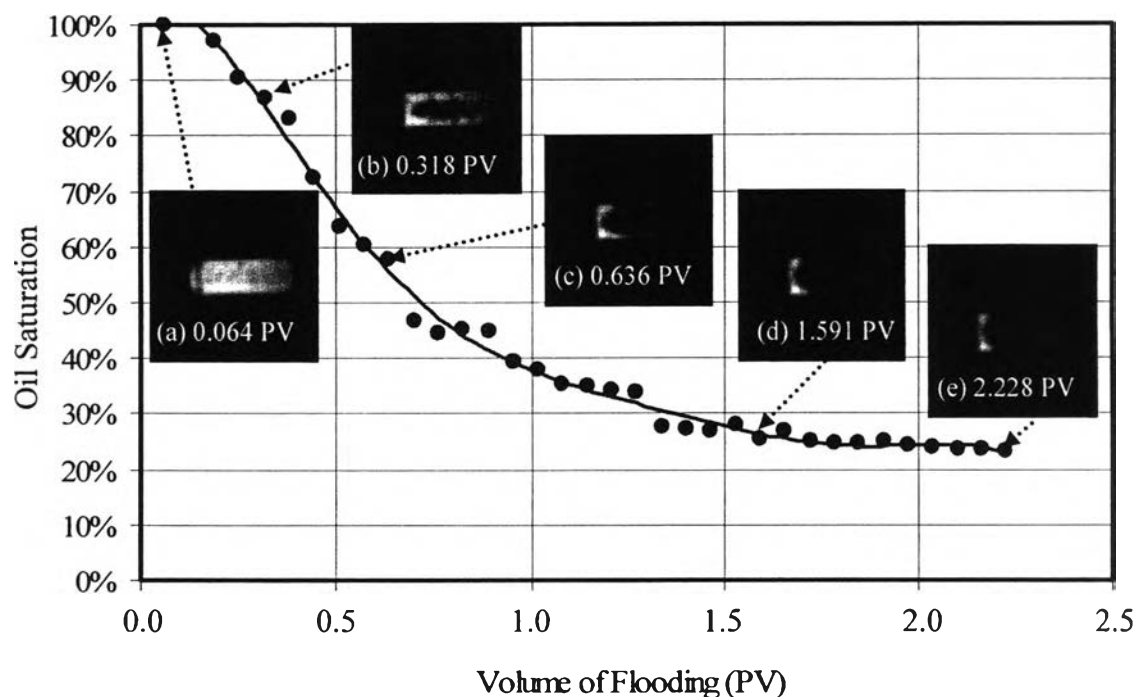
The FS-5 was used as the oil phase and deionized water was used during waterflooding process. The oil viscosity to water viscosity ratio,  $\mu_o/\mu_w$ , is 25.8 at 25°C. This oil/water viscosity ratio is  $> 1$  which leads to an unstable displacement ( $M > 1$ ). The interfacial tension between deionized water and oil was 43.5 dynes/cm. Material balances and MRI were used in these experiments to monitor the efficiency of flooding process.

In situ permeability-modification processes were investigated in Channel sample # 2 and Channel sample # 3. Cr(III)-carboxylate/acrylamide-polymer (CC/AP) gel was applied. This gel contained 0.75 wt% of HPAM and 0.3 wt% of Cr(III) acetate. The gelation times were 12 hours and 48 hours at 40°C for Channel sample # 2 and Channel sample # 3, respectively.

#### 4.5.1 No channel sample

The first experiment was conducted without a channel as a reference experiment. The waterflooding experiment of unconsolidated homogeneous fine sand was used to compare with other heterogeneous samples (a high-permeability channel in sand pack samples). Since the fine sand was used, the properties of the sand pack sample before the flood testing were different from previous experiments. The sample had a pore volume of 12.62 ml, porosity of 33.95% and permeability of 10,460 mD. The experiment was conducted at room temperature ( $\sim 25^\circ\text{C}$ ).

An initial oil saturation of 90.75 % was observed before the waterflooding process. The injection of 28.11 ml of water (2.23 PV) at a constant flow rate of 0.06 ml/min was used. Figure 4.11 shows the oil saturation profile from the integral total MRI signal and acquired images through the waterflooding process.



**Figure 4.11** Residual oil saturation ( $S_{or}$ ) profile and images for No channel sample

Figure 4.11 (a) shows the porous media after the injection of 0.064 PV. The image shows a high intensity, which is equivalent to oil saturation in the sand pack. Then, as water displaced oil in the porous media, a more unstable displacement front was developed. In Figure 4.11 (b), the channeling and/or fingering (the unfavorable water displacement front) of water (dark areas) was clearly detected as well as pockets of by-passed oil (white or bright areas) left behind the waterflooding front. After water injection of 0.636 PV, the formation of a well-defined water channel (viscous fingering) from the injection point to the producer end can be observed. However, the vertical sweep was improved (towards the upper and lower vertical edges of the sand pack) as the displacement process advanced stabilizing the viscous fingering in the volumetric sense, consequently a uniform displacement front was developed.

The high signal of oil left behind a fluid diffuser plate at the inlet-face of the sand pack was detected. Since the edge of the fluid diffuser plate was sealed with the syringe, the convex displacement front was formed. This remaining oil was observed

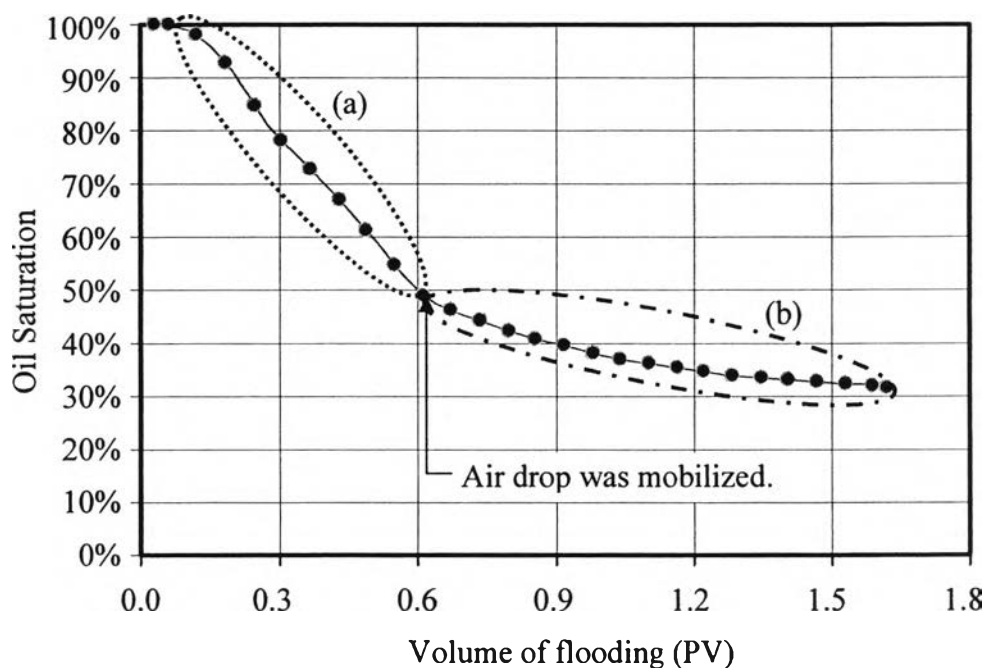
in every experiment for the channel system which corresponded to residual oil saturation.

The oil saturation profile in Figure 4.11 corresponds to the direct monitoring of the waterflooding process using MRI. The residual oil saturation ( $S_{or}$ ) determined by MRI was 23.3 %. While residual oil saturation, based on material balance was 21.1 %. These  $S_{or}$  show a close agreement between MRI technique and material balance (2.2 % difference).

#### **4.5.2 Channel sample # 1: Effect of air drop in the channel**

In this experiment, waterflooding was conducted in a sand pack having a high-permeability channel, as indicated in Figure 4.10. In this sample preparation, the channel inlet was covered to prevent water and/or oil passing through the channel. The matrix properties of this sample were measured i.e. pore volume of 13.12 ml, porosity of 34.02 % and permeability of 13,670 mD. The permeability of the channel was estimated using Poiseuille's law for capillary flow combined with Darcy's law for flow of liquids in permeable beds. From the calculations, the glass channel had a permeability of 163,990 Darcys and the average permeability of the channel/matrix system was 1,296 Darcys. The experiment was carried out at room temperature ( $\sim 25^\circ\text{C}$ ).

An initial oil saturation of 88.84 % in the sand matrix before the waterflooding process was measured. Then, the channel inlet was opened to show the effect of the high-permeability zone through the waterflooding process. Since the channel was full of air,  $0.4\text{ cm}^3$  of oil (channel volume) was injected to fill the channel with oil. Some bubbles of air were released from the channel. At this point, the waterflooding was ready to start. A volume of 21.28 ml of water (1.62 PV) was injected at a constant flow rate of 0.06 ml/min.

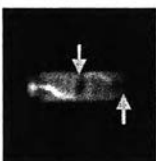


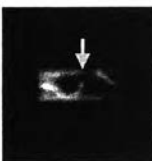

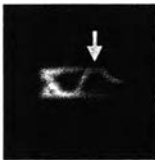
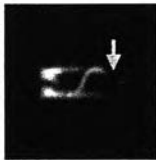




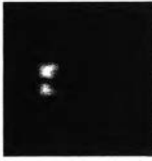


**Figure 4.12** Residual oil saturation ( $S_{or}$ ) profile from MRI for Channel sample # 1

Figure 4.12 shows the oil saturation profile from the integral total MRI signal. The acquired images through the waterflooding process which correspond to Figure 4.12 are shown in Table 4.9. It is expected that an unstable displacement front should develop and this can be observed from images since the waterflooding displacement was far from having mobility-control in addition to the existence of a high-permeability channel.

In this experiment, an interesting feature of air drop trapping and mobilization was directly visualized in-situ by MRI. The effect of these processes on oil recovery was clearly shown from the residual oil saturation profile. From Table 4.9, the first image of 0.061 PV shows the initial stage of the sand pack and the channel. From this image, the sand matrix and the channel were essentially saturated with oil. However, the presence of the air drops in the middle and outlet end of the channel were detected (as indicated by arrows in the first image).

**Table 4.9** Images of porous media during waterflooding for Channel sample # 1

| Corresponding to | Images at each PV                                                                 |                                                                                    |                                                                                    |                                                                                     |                                                                                      |
|------------------|-----------------------------------------------------------------------------------|------------------------------------------------------------------------------------|------------------------------------------------------------------------------------|-------------------------------------------------------------------------------------|--------------------------------------------------------------------------------------|
| Figure 4.12 (a)  |  |   |  |  |                                                                                      |
|                  | 0.061                                                                             | 0.122                                                                              | 0.306                                                                              | 0.459                                                                               |                                                                                      |
|                  |  |   |  |  |                                                                                      |
|                  | 0.490                                                                             | 0.520                                                                              | 0.551                                                                              | 0.582                                                                               |                                                                                      |
|                  | Figure 4.12 (b)                                                                   |  |  |  |  |
|                  |                                                                                   | 0.612                                                                              | 0.643                                                                              | 0.918                                                                               | 1.622                                                                                |

The air drop trapping in the middle of the channel has an the important role in this experiment. Since the air drop was trapped in the channel, there was no water flow through the channel until capillary forces are overcome to mobilize the drop. The injected water was diverted from the high-permeability zone to the sand matrix. At 0.122 PV of flooding, the channel was still saturated with oil (bright areas) while the oil in the sand matrix was beginning to be displaced (dark areas of water saturation in the middle of the sand matrix). However, the trapped drop was continuously mobilized as indicated by an arrow in the image. Then, more oil in the sand matrix was flooded by water but the condition of the capillary remained the same as before.

The capillary forces within the channel were overcome at 0.551 PV. As a result of this, the injected water invaded the high-permeability channel and the mobilization of the air drop was initiated. The oil in the channel was displaced after this point. At 0.612 PV, an entirely new process took place during this waterflooding. Injected water at this point flowed preferentially through the high-permeability channel. The oil saturation profile confirmed that once the trapped drop was mobilized

and the oil in the channel was displaced at 0.612 PV, this profile changed slightly compared with the first part of flooding (Figure 4.12 (a)). From the residual oil saturation profile in the second part of the flooding (Figure 4.12 (b)), the oil recovery leveled off and the residual oil saturation in the model sand pack did not change in a significant manner even after injecting more than twice the pore volume of water (from 0.612 to 1.622 PV).

At the end of the waterflooding, after the injection of 1.622 PV, the image shows that the channel was completely saturated with water (totally dark signal from the channel). The remaining oil in the sand matrix behind the fluid diffuser plate at the inlet-face of the sand pack was observed. As mentioned in the previous experiment, this oil was the majority of residual oil left in the sample.

The MRI residual oil saturation at the end of waterflooding was 31.7 % (refer to Figure 4.12) and the residual oil saturation,  $S_{or}$ , calculated from the material balance was 27.1 %. Once more, fluid saturations estimated through MRI shows an agreement with material balance (4.6 % difference).

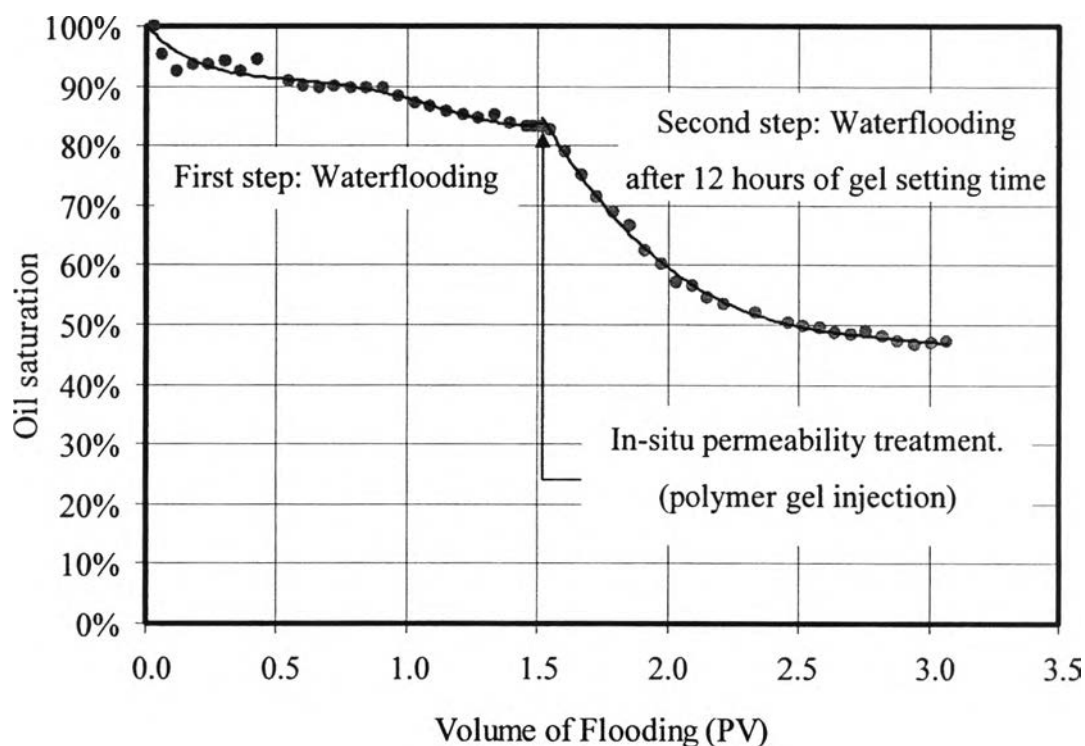
#### 4.5.3 Channel sample # 2: Effect of irreducible water saturation

Application of the polymer gel treatment was undertaken in this sample. Two waterflooding displacement steps were conducted. The in-situ permeability treatment aimed to improve the substantial variation of the water injection flow pattern due to the existence of a high-permeability channel. Before the flooding experiment, the pore volume of 13.22 ml, porosity of 34.28 % and permeability of 12,260 mD were measured in the sand matrix. Since the same channel as in Channel sample # 1 was used, the channel had the permeability of 163,990 Darcys as before. The average permeability of 1,295 Darcys for the channel/matrix system was calculated. The experiment was conducted at room temperature ( $\sim 25$  °C).

The sample was prepared without covering the channel inlet; therefore, the water and/or oil passed through the channel from the beginning of this experiment. The subsequent step in the preparation of the sand pack was the drainage of the sample using Fluorolube FS-5 until the irreducible water saturation ( $S_{wirr}$ ) was reached. An initial oil saturation in the sample was calculated. Since the channel inlet was opened, the oil passed through the channel and saturated only the first-half length of





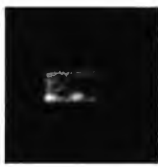



the sand matrix. The initial oil saturation in the matrix before the waterflooding process was only 44.28 %.

MRI allowed the direct and in-situ visualization of CC/AP gel treatment on oil displacement and recovery. Gel was applied to the channel for 12 hours gel setting time in order to plug the channel during the first and second steps of waterflooding. The oil saturation profile for these two steps is shown in Figure 4.13. The images from MRI for both steps, which correspond to Figure 4.13 are shown in Table 4.10.



**Figure 4.13** Residual oil saturation ( $S_{or}$ ) profile from MRI for Channel sample # 2

**Table 4.10** Images of porous media during waterflooding for Channel sample # 2

| Corresponding to                                                       | Images at each PV                                                                          |                                                                                            |                                                                                             |                                                                                              |
|------------------------------------------------------------------------|--------------------------------------------------------------------------------------------|--------------------------------------------------------------------------------------------|---------------------------------------------------------------------------------------------|----------------------------------------------------------------------------------------------|
| First step:<br>Waterflooding                                           | <br>0.030 | <br>0.091 | <br>1.032 | <br>1.488 |
| Second step:<br>Waterflooding<br>after 12 hours<br>of gel setting time | <br>1.518 | <br>1.731 | <br>2.217 | <br>3.067 |

In the first step of waterflooding, the injection of 19.67 ml of water (1.49 PV) at a constant flow rate of 0.06 ml/min was used. The first image at 0.030 PV was taken at the beginning of the waterflooding. This image shows that the first half of the sample and the channel were saturated with oil, while the other part was saturated with connate water. As the waterflooding advanced, the water channeled through the high-permeability pathway. A significant amount of oil was left behind in the sand matrix. From 0.091 PV to 1.488 PV, the images illustrated that this waterflooding displacement is inefficient and the first half of the sand unit contains the majority of the residual oil. As shown in Figure 4.13, the oil saturation profile from MRI indicates that the residual oil saturation after the first waterflooding displacement was 83.2 %. Therefore, the injection of 1.49 PV of water displaced only 16.8 % of the original oil in place for a high-permeability channel system.

After the first waterflooding displacement, an in-situ permeability reduction treatment was applied using a CC/AP gel. The gel was formulated and immediately injected into the high-permeability channel using a syringe. A period of 12 hours was allowed for gel setting at a temperature of 40 °C. The gel is essentially immobile and thus acts to reduce the apparent permeability of the rock matrix or fracture (Green and Willhite, 1988). In this type of treatment, selective application into a high-



permeability channel is essential in order to make sure that other areas of the sand matrix are not affected by the gel treatment.

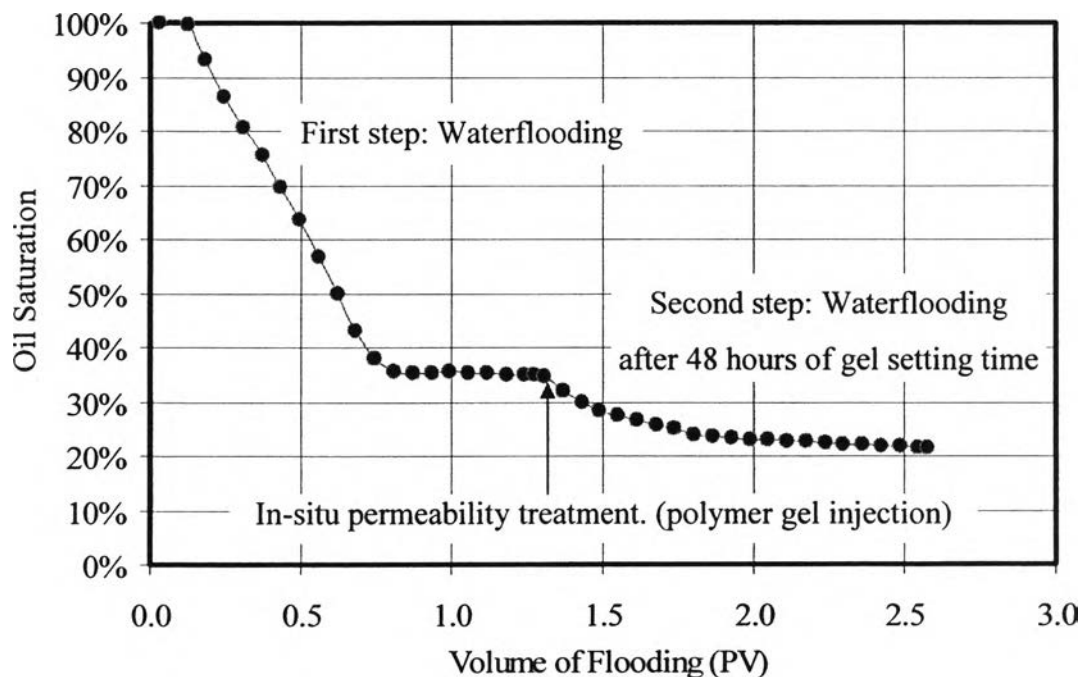
In the second step of waterflooding after 12 hours of gel application, the injection of 20.88 ml of water (1.58 PV) at the same constant flow rate of 0.06 ml/min was used. The images for this experiment were started from 1.518 PV to 3.067 PV as shown in Table 4.10 (these numbers included the amount of water injection in the first waterflooding experiment). The first image at 1.518 PV shows the sample right after gel treatment application, the oil content in the sample was close to the last image from the first experiment (1.488 PV). As the water displacement process advanced, more oil in the sand matrix was displaced. The images indicate that a more stable displacement front was developed. This is evident from the more uniform MRI dark signals observed from 1.731 PV to 3.067 PV. The last image at 3.067 PV shows the residual oil left behind the fluid diffuser plate at the inlet-face of the sand pack. The second part of the oil saturation profile from MRI dramatically declined since the injected water was diverted towards the lower permeability zones (the sand matrix). The MRI residual oil saturation decreased from 83.2 % to 47.1 % (36.1 % additional oil recovery after the permeability modification treatment). The total residual oil saturation,  $S_{or}$ , calculated from material balance was 38.3 %. The deviation between the residual oil saturation determined by MRI and mass balance was 8.8 %. This deviation could be caused by MRI tuning differences during the displacement experiments since the total experiment time was two days.

#### **4.5.4 Channel sample # 3: Effect of oil drop in the channel**

Two waterflooding displacement steps were conducted, separated by the application of 48 hours polymer gel treatment. The double gel setting time of Channel sample # 2 was used to evaluate the effect of gel strength on oil recovery. Before the flooding experiment, the channel inlet was sealed to avoid the large amount of irreducible water saturation at the outlet of the sample. The properties of the sand matrix i.e. the pore volume of 12.92 ml, porosity of 33.51 % and permeability of 13,167 mD were measured. The same channel as in previous experiments with a permeability of 163,990 Darcys was used. The average permeability for the chan-





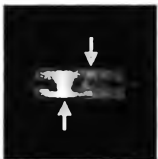





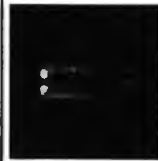

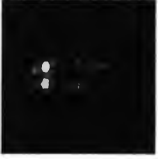

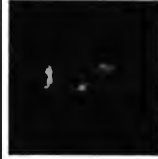

nel/matrix system was 1,296 Darcys. The experiment was conducted at room temperature ( $\sim 25^\circ\text{C}$ ).

An initial oil saturation in the sand matrix before the waterflooding process was 90.18 %. The channel inlet was opened and followed by the injection of  $0.4\text{ cm}^3$  of oil (channel volume). The first image of the sample was taken before the waterflooding process in order to make sure that the channel was full of oil and no air drop was trapped inside the channel. The oil saturation profile for both steps of waterflooding (before and after 48 hours) is shown in Figure 4.14. The images from MRI which correspond to Figure 4.14 are presented in Table 4.11. This experimental outcome demonstrates that MRI is a convenient and useful tool to visualize the occurrence of in-situ events within the porous media. This technique allows a better interpretation and understanding of the process due to the direct visualization of the flooding experiment.



**Figure 4.14** Residual oil saturation ( $S_{or}$ ) profile from MRI for Channel sample # 3

**Table 4.11** Images of porous media during waterflooding for Channel sample # 3

| Corresponding to                                                       | Images at each PV                                                                   |                                                                                     |                                                                                      |                                                                                       |
|------------------------------------------------------------------------|-------------------------------------------------------------------------------------|-------------------------------------------------------------------------------------|--------------------------------------------------------------------------------------|---------------------------------------------------------------------------------------|
| First step:<br>Waterflooding                                           |    |    |    |    |
|                                                                        | 0.031                                                                               | 0.093                                                                               | 0.155                                                                                | 0.187                                                                                 |
|                                                                        |    |    |    |    |
|                                                                        | 0.249                                                                               | 0.311                                                                               | 0.497                                                                                | 0.684                                                                                 |
|                                                                        |   |   |   |   |
|                                                                        | 0.746                                                                               | 0.777                                                                               | 0.932                                                                                | 1.243                                                                                 |
| Second step:<br>Waterflooding<br>after 48 hours<br>of gel setting time |  |  |  |  |
|                                                                        | 1.305                                                                               | 1.554                                                                               | 1.865                                                                                | 2.579                                                                                 |

The water injection of 16.06 ml of water (1.24 PV) at a constant flow rate of 0.06 ml/min was used in the first step of waterflooding. The first image at 0.031 PV shows that the channel was completely saturated with oil. Once waterflooding was initiated, the injected water rapidly channeled through the high-permeability zone. However, two oil drops were trapped inside the channel as indicated from 0.155 PV to 0.249 PV. The pressure required to overcome capillary forces and mobilize the trapped oil drops was significant. Under the experimental conditions, the injected water did not flow through the channel. The water was diverted towards the lower permeability areas of the sand matrix instead. The capillary forces from the oil drop as indicated by the arrows from 0.311 PV to 0.684 PV prevented water channeling

through the high-permeability zone. At 0.746 PV, the capillary forces within the channel were overcome. The image shows that the oil drop was moved (as indicated by the arrow at 0.746 PV) and the breakthrough saturation was reached. Figure 4.14 shows that the profile suddenly becomes steady and the residual oil saturation is attained after this point. The MRI residual oil saturation was 34.8 % at the end of the first waterflooding displacement (1.24 PV of water injection).

After the first waterflooding was terminated, the CC/AP gel was applied to the channel as an in-situ permeability reduction treatment. A period of 48 hours for gel setting at a temperature of 40°C was allowed. This was followed by the injection of 17.26 ml of water (1.34 PV) at the same constant flow rate of 0.06 ml/min. The water injection started from 1.305 PV to 2.579 PV; these include the amount of injected water in the first waterflooding experiment. The image at 1.305 PV shows the sand pack immediately after the gel treatment, which is the beginning of the second waterflooding stage. The remaining oil in the sand matrix behind the fluid diffuser plate at the inlet-face of the sand pack can be observed. Some oil is also observed in the channel at the same locations of the trapped oil drops from the previous waterflooding step. From the images and oil saturation profile in the second step, some oil that was left behind in the sand matrix was gradually displaced by water. The sweep efficiency was improved and the oil recovery was increased after gel treatment. At the last image (2.579 PV), only a small amount of oil was observed in the sand unit.

The MRI residual oil saturation was decreased from 34.8 % to 21.5 %, which indicated an additional oil recovery of 13.3 %. The total residual oil saturation,  $S_{or}$ , calculated from a material balance was 21.6 %. The MRI tuning was adjusted to achieve a better signal in the second stage of experiment. This improved the quantitative estimation from MRI. The fluid saturations estimated through MRI shows a close agreement with the material balance (0.1 % difference).

#### 4.5.5 Comparison of the channel system

Four waterflooding experiments in channel system were conducted which consisted of waterflooding in an unconsolidated sand pack without a channel (No Channel sample) and 3 unconsolidated sand packs having high permeability channel (Channel sample # 1, # 2, and # 3). CC/AP gel was applied with the gelation times of

12 hours and 48 hours at 40 °C for Channel sample # 2 and Channel sample # 3 respectively. Table 4.12 shows the properties of the channel samples before the flood testing, i.e. pore volume, porosity, and permeability in matrix, channel, and average (matrix and channel). The average pore volume and porosity for the four samples were 12.97 ml and 33.94 %, respectively. The permeability of the samples in channel system were calculated by using Poiseuille's law for capillary flow combined with Darcy's law for flow of liquids in permeable beds as described in Chapter 2. An average matrix permeability of 12,390 mD, channel permeability of 163,990 Darcys, and an average permeability of the unconsolidated matrix/channel system of 1,296 Darcys were used in this study. All experiments were conducted at room temperature (~25 °C).

**Table 4.12** Properties of sand pack sample before flood testing for channel system

| Channel sample | Pore Volume (ml) | Porosity       | Permeability (Darcys) |                |                              |
|----------------|------------------|----------------|-----------------------|----------------|------------------------------|
|                |                  |                | Matrix                | Channel        | Average (Matrix and channel) |
| No Channel     | 12.62            | 33.95 %        | 10.46                 | -              | -                            |
| Channel # 1    | 13.12            | 34.02 %        | 13.67                 | 163,990        | 1,296                        |
| Channel # 2    | 13.22            | 34.28 %        | 12.26                 | 163,990        | 1,295                        |
| Channel # 3    | 12.92            | 33.51 %        | 13.17                 | 163,990        | 1,296                        |
| <b>Average</b> | <b>12.97</b>     | <b>33.94 %</b> | <b>12.39</b>          | <b>163,990</b> | <b>1,296</b>                 |

The comparison in terms of the oil saturation before flooding and the residual oil saturation is considered only for No Channel sample, Channel sample # 1, and Channel sample # 3. Since the sand pack preparation part for Channel sample # 2 was different. The channel inlet was opened from the beginning of the displacement process for this experiment. It led to the large amount of irreducible water saturation at the outlet of the sample. The residual oil saturation at the end of the waterflooding process revealed a significant deviation of 8.8 % between the material balance and

integral total MRI signal from Channel sample # 2. In this displacement test, the MRI tuning was also changed due to the length of the experiment.

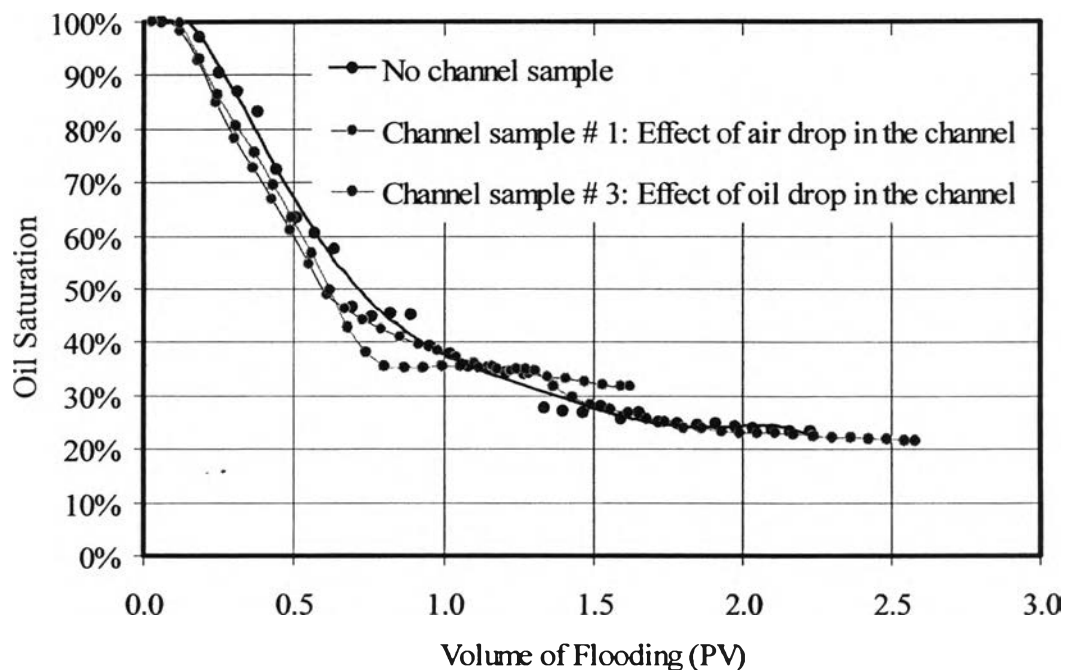
The water-wet sand of the matrix in the channel system was the fine sand (grain size diameter of 0.417 mm to 0.150 mm). The average oil saturation in the matrix before flooding (without Channel sample # 2) was 89.92 vol%.

**Table 4.13** Oil saturation, Volume of flooding and Residual oil saturation ( $S_{or}$ ) after flood testing for channel system

| Channel system | Oil saturation before flooding | Total volume of flooding | Residual oil saturation ( $S_{or}$ ) |                  | % Deviation |
|----------------|--------------------------------|--------------------------|--------------------------------------|------------------|-------------|
|                |                                |                          | Material balance                     | Imaging from MRI |             |
| No Channel     | 90.75 vol%                     | 28.11 ml,<br>2.23 PV     | 21.1 %                               | 23.3 %           | 2.2 %       |
| Channel # 1    | 88.84 vol%                     | 21.28 ml,<br>1.62 PV     | 27.1 %                               | 31.7 %           | 4.6 %       |
| Channel # 2    | 44.28 vol%                     | 40.55 ml,<br>3.07 PV     | 38.3 %                               | 47.1 %           | 8.8 %       |
| Channel # 3    | 90.18 vol%                     | 33.32 ml,<br>2.58 PV     | 21.6 %                               | 21.5 %           | 0.1 %       |

Figure 4.15 shows the comparison of the residual oil saturation profile ( $S_{or}$ ) from MRI (considered only No Channel sample, Channel sample # 1, and Channel sample # 3). The first displacement sand pack test (No Channel) was conducted as a reference experiment. In this case, the injection of 2.23 PV of water displaced 76.7% of oil, leaving a residual oil saturation of 23.3%. Trapping of nonwetting phase in capillary channel or Jamin effect was detected in both Channel sample # 1 and Channel sample # 3. In Channel sample # 1, the effect of an air drop in the channel was observed. It was noticed that, the injection of 0.55 PV of water was required to overcome the capillary force within the channel to mobilize the air drop. The total

volume of water injected in this experiment was 1.62 PV resulting in a residual oil saturation of 31.7 %. The last experiment, Channel sample # 3, presented the effect of an oil drop in the channel on oil distribution and the effect of in-situ modification treatment by using CC/AP gel to block the channel. Therefore, this experiment was divided into two steps. In the first step, the oil drop was mobilized after the injection of 0.75 PV of water. The residual oil saturation was 34.8 % at the end of the first step of waterflooding (1.24 PV of water injection). The second step, after applying CC/AP gel at 40°C for 48 hours, the final residual oil saturation was 21.5 % with the total volume of water injected being 2.58 PV.



**Figure 4.15** Comparison of residual oil saturation ( $S_{or}$ ) profile from MRI for channel system

The different amounts of water in order to mobilize fluids trapped in the capillary channel for Channel sample # 1 and Channel sample # 3 is significant. This reflects the effects of wettability between nonwetting phase trapped in capillary channel and capillary glass channel surface as well as the interfacial tension between displacing phase (water) and displaced phase in the channel (the air drop in Channel sample # 1 and the oil drop in Channel sample # 3). The injected water required to

overcome the capillary pressure within the capillary channel for Channel sample # 1 is less than Channel sample # 3. Therefore, the capillary force required to overcome an oil drop is higher than an air drop since the oil phase wetted a glass surface better than the air. Without the in-situ modification, the residual oil saturation is about 33 % for both air/oil drop effects in the channel system. Nevertheless, with the CC/AP gel treatment, incremental oil is recovered. An approximate residual oil saturation of 22% is reached for both a No Channel sample and Channel sample # 3 after CC/AP gel application.

The results obtained indicated the usefulness of the Centric Scan SPRITE MRI technique to study oil displacement processes. This technique constitutes an important imaging tool for the direct and quantitative evaluation of the waterflooding process and monitoring of the application of CC/AP gel as a permeability modification treatment in a high-permeability channel for the enhanced recovery of oil in unconsolidated porous media. It is anticipated that similar results would be obtained using consolidated porous media of significantly lower permeabilities.